Statistical mechanics of kinks in 1+1 dimensions: Numerical simulations and double-Gaussian approximation

Francis J. Alexander,[1,*] Salman Habib,[2,†] and Alex Kovner[3,‡]

[1]*Center for Nonlinear Studies, Los Alamos National Laboratory, Los Alamos, New Mexico 87545*
[2]*T-6, Theoretical Division, Los Alamos National Laboratory, Los Alamos, New Mexico 87545*
[3]*T-8, Theoretical Division, Los Alamos National Laboratory, Los Alamos, New Mexico 87545*

We investigate the thermal equilibrium properties of kinks in a classical Φ^4 field theory in 1+1 dimensions. From large-scale Langevin simulations we identify the temperature below which a dilute-gas description of kinks is valid. The standard dilute-gas or WKB description is shown to be remarkably accurate below this temperature. At higher "intermediate" temperatures, where kinks still exist, this description breaks down. By introducing a double-Gaussian variational ansatz for the eigenfunctions of the statistical transfer operator for the system, we are able to study this region analytically. In particular, our predictions for the number of kinks and the correlation length are in agreement with the simulations. The double Gaussian prediction for the characteristic temperature at which the kink description ultimately breaks down is also in accord with the simulations. We also analytically calculate the internal energy and demonstrate that the peak in the specific heat near the kink characteristic temperature is indeed due to kinks. In the neighborhood of this temperature there appears to be an intricate energy-sharing mechanism operating between nonlinear phonons and kinks.

PACS number(s): 05.20.−y, 11.10.−z, 63.75.+z

I. INTRODUCTION

The equilibrium and nonequilibrium statistical mechanics of solitons, solitary waves, and other coherent structures in nonlinear systems has been a subject of study for some time [1]. Recent interest has been fueled by new applications not only in condensed-matter physics [2,3], but also by potential applications in particle physics (sphalerons) [4] and cosmology (domain walls, baryogenesis) [5].

In this paper we focus on the classical equilibrium statistical mechanics of solitary wave ("kink") solutions of a tachyonic mass, Φ^4 ("double-well") field theory in 1+1 space-time dimensions with the Lagrangian density

$$L = \tfrac{1}{2}(\partial_t \Phi)^2 - \tfrac{1}{2}(\partial_x \Phi)^2 + \tfrac{1}{2}m^2\Phi^2 - \tfrac{1}{4}\Lambda\Phi^4 , \tag{1}$$

and the corresponding equation of motion

$$\partial_{tt}^2 \Phi = \partial_{xx}^2 \Phi + m^2\Phi - \Lambda\Phi^3 . \tag{2}$$

This model is of direct relevance to the study of displacive phase transitions [6] and magnetic spin chains [7]. Moreover, the behavior of this model is representative of a large class of soliton-bearing systems. Finally, it has the added advantage of being amenable to both theoretical analysis and numerical simulation.

The kink solution of the equation of motion (2) is the localized field configuration that interpolates between the two asymptotic field potential-energy minima at $\Phi = \pm\Phi_0 = \pm m/\sqrt{\Lambda}$. Kink solutions of the field equations are inaccessible to perturbation theory: A statistical mechanics of kinks is nevertheless still possible, partly because they are localized objects. The static kink solution centered at $x = x_0$ is

$$\Phi_k = \frac{m}{\sqrt{\Lambda}}\tanh\left[\frac{m}{\sqrt{2}}(x - x_0)\right] , \tag{3}$$

and the negative of the kink solution is the antikink. Since the Lagrangian (1) is Lorentz invariant, time-dependent solutions are easily found by boosting the static solution. The energy density of the static kink (or antikink) is

$$\varepsilon_k(x) = \frac{m^4}{2\Lambda}\operatorname{sech}^4\left[\frac{m(x - x_0)}{\sqrt{2}}\right] , \tag{4}$$

from which the total energy of an isolated kink, or the kink mass, is obtained,

$$E_k = \int_{-\infty}^{+\infty} dx\, \varepsilon_k(x) \tag{5}$$

$$= \sqrt{(8/9)}\frac{m^3}{\Lambda} . \tag{6}$$

In numerical simulations it is customary to employ a dimensionless form of the theory given by the transformations:

$$\phi = \Phi/a ,$$

$$\bar{x} = mx , \tag{7}$$

$$\bar{t} = mt ,$$

where $a^2 = m^2/\Lambda$. Applying these transformations, we

*Electronic address: fja@goshawk.lanl.gov
†Electronic address: habib@eagle.lanl.gov
‡Electronic address: kovner@pion.lanl.gov

have

$$H = ma^2 \bar{H} , \tag{8}$$

where H is the original field Hamiltonian, and

$$\bar{H} = \int d\bar{x} \left[\tfrac{1}{2} \bar{\pi}^2 + \tfrac{1}{2} (\bar{\nabla}\phi)^2 - \tfrac{1}{2}\phi^2 + \tfrac{1}{4}\phi^4 \right] . \tag{9}$$

The new field ϕ satisfies the equation of motion

$$\partial_{tt}^2 \phi = \partial_{\bar{x}\bar{x}}^2 \phi - \phi(\phi^2 - 1) . \tag{10}$$

We enforce $\bar{\beta}\bar{H} = \beta H$ by introducing a new scaled temperature $\bar{\beta} = \beta/(ma^2)$.

The statistical mechanics of kinks in this system has been studied by two approaches. In the first, and phenomenological, approach one assumes that the kinks and the field fluctuations about the asymptotic field minima ("phonons") may be treated as weakly interacting elementary excitations. Provided that the kink density is low (the dilute-gas approximation), the canonical partition function can be found by standard methods [1,8,9]. Alternatively, as shown by Krumhansl and Schrieffer (KS) [8], building on earlier work of Scalapino, Sears, and Ferrell [10], it is possible to calculate the partition function, in principle exactly, by exploiting a transfer operator technique. KS showed that in the low-temperature (dilute-gas) limit the partition function naturally factorizes into two contributions both having counterparts in the phenomenological theory; a tunneling term which they were able to identify with the kink contribution, and the remainder which they identified as the linearized phonons. The approach of KS was further refined and extended to a wider class of systems by Currie et al. [9]. In this work, interactions of kinks with linearized phonons were taken into account, leading to substantial corrections to the results of KS.

The key result of these efforts is the prediction that, below a certain temperature, the spatial density of kinks is

$$n_k \propto \sqrt{E_k \beta} \exp(-E_k \beta) . \tag{11}$$

A related prediction is that the field correlation length λ defined by

$$\langle \Phi(0)\Phi(x) \rangle \sim \exp(-|x|/\lambda) \tag{12}$$

exhibits an exponential temperature dependence [9],

$$\lambda = \frac{1}{4}(\pi/3) \frac{1}{\sqrt{E_k\beta}} \exp(E_k\beta) \tag{13}$$

at low temperatures.

Computer simulations to verify these results date back to Ref. [11] where only a qualitative agreement was found. Recent work [12–15] has led to more detailed comparisons, however significant discrepancies have been reported. This has led to theoretical speculation [16,17] regarding possible corrections to the dilute-gas theory of kinks. It has been suggested that these discrepancies are due to finite-size effects and phonon dressing of the bare kink energy (breather contributions to the free energy may also be significant [18]). As was discussed in Ref.

[19], the earlier simulations were not carried out at low enough temperatures: Nevertheless the authors interpreted their results in terms of WKB formulas that are simply not a valid description over the range of temperatures they had studied. In this intermediate-temperature regime, there is no unique characterization of what constitutes a kink and how to differentiate it from a nonlinear phonon. By going to low enough temperatures where the dilute gas results are valid, we are also able to rule out an earlier claim of substantial phonon dressing even at these temperatures [11].

We have numerically studied the equilibrium statistical mechanics of kinks in the Φ^4 model by implementing a Langevin code on a massively parallel computer. To understand our results in the high- and intermediate-temperature region not susceptibile to a dilute-gas analysis, we have used a nonperturbative double Gaussian wave function approximation in the quantum-mechanical problem for determining the eigenvalues of the transfer operator. The study of the intermediate temperature regime is important because kink contributions to some thermodynamic quantities (e.g., the specific heat) of the system may be dominant precisely in this region. Numerical calculations of the partition function, while certainly valuable, are by themselves not sufficient. Such calculations, for example, cannot explain the nature of the peak in the specific heat nor can they enable one to extract which effects are due to kinks and which effects are due to phonons.

Stated in brief, our results are the following: (1) the dilute-gas predictions for the kink density and the correlation length are very accurate below a certain (theoretically estimable) temperature; (2) above this temperature the Gaussian results for the kink number and correlation length agree with the simulations; (3) kinks are found to "disappear" into the thermal phonon background above a characteristic temperature, in good agreement with our theoretical prediction; (4) our Gaussian approximation accurately describes the classical single-point field distribution function at high and intermediate temperatures where the dilute-gas (WKB) approximation breaks down; and (5) the internal energy and the specific heat calculated in double-Gaussian approximation show an interesting energy sharing process between kinks and nonlinear phonons in an intermediate-temperature range below the characteristic temperature at which kinks appear: a peak in the specific heat in this temperature range is shown to be due essentially to kinks.

The rest of this paper is organized as follows. We describe our computer simulation and numerical techniques in Sec. II. Section III is a brief review of the transfer operator formalism and the standard WKB results for the partition function. Here we also introduce an "effective" definition of the kink number that takes into account an averaging over the thermal phonon length scale. In Sec. IV we introduce the double-Gaussian variational method and use it to find approximate eigenfunctions and eigenvalues of the transfer operator and also to compute thermodynamic quantities such as the specific heat. Finally, we conclude in Sec. V with a discussion of our results and of directions for future work.

II. THE SIMULATIONS

The Langevin equation for the dimensionless theory is

$$\partial^2_{\bar{t}\bar{t}}\phi = \partial^2_{\bar{x}\bar{x}}\phi - \eta\partial_{\bar{t}}\phi + \phi(1-\phi^2) + F(\bar{x},\bar{t}) . \qquad (14)$$

To guarantee an approach to equilibrium, the Gaussian, white noise F, and the viscosity η are related via the fluctuation-dissipation theorem

$$\langle F(\bar{x},\bar{t})F(\bar{y},\bar{s})\rangle = 2\eta\bar{\beta}^{-1}\delta(\bar{x}-\bar{y})\delta(\bar{t}-\bar{s}) . \qquad (15)$$

Since in this paper we are interested only in the equilibrium properties of the system which are independent of the viscosity, we fixed $\eta=1$ for all the simulations. (It was verified that the results did not depend on the value of η.)

We carried out numerical simulations of this Langevin equation using a standard first-order Euler differencing technique. The second order in time Langevin equation (14) was written as the two first-order finite difference equations

$$v(\bar{t}+\epsilon) = v(\bar{t}) + \epsilon\{[\bar{\phi}(\bar{x}+\delta) + \bar{\phi}(\bar{x}-\delta) - 2\bar{\phi}(\bar{x})]/\delta^2$$
$$-\eta v(\bar{t}) + \bar{\phi}(\bar{x})[1-\bar{\phi}^2(\bar{x})] + F(\bar{x},\bar{t})\} ,$$

$$\bar{\phi}(\bar{t}+\epsilon) = \bar{\phi}(\bar{t}) + \epsilon v(\bar{t}+\epsilon) , \qquad (16)$$

where the "velocity" $v=\partial_{\bar{t}}\bar{\phi}$. The finite differencing was implemented with a time step $\epsilon=0.02$, and a lattice spacing $\delta=0.5$. The space-time noise was generated by summing N random variables uniformly distributed over $(-0.5,0.5)$. From the central limit theorem, in the limit that $N\to\infty$ this sum should approach a Gaussian random variable with mean 0 and variance $\sqrt{N}/12$. For convenience we chose $N=12$: since this gave a noise normalized to a strength of unity, for each given temperature the normalization was straightforwardly determined by the fluctuation-dissipation relation. The results presented here were obtained on lattices consisting of 16 384 sites and we have checked their consistency with results from lattices of different sizes. The lattice volume is large enough that there are no discernible finite-size effects.

Our system size is one to two orders of magnitude larger than that in most previous simulations. Large system sizes are necessary to get acceptable statistics at low temperatures. In many of the recent numerical simulations of this model, the system size was such that only a few kinks would appear at the lowest temperatures studied. For temperatures in the range where the WKB theory is valid, on average fewer than one kink would appear on systems of the sizes used in Refs. [12–15].

The lattice systems were evolved from random initial configurations to equilibrium. The length of time necessary to ensure equilibrium increased with inverse temperature. For $\bar{\beta}=8$ the time required was approximately 10^7 time steps, and for the highest temperatures, less than 10^5 steps.

Two quantities of interest reported here are the kink number and the field correlation length. To compute the kink number, we need an operational way to identify kinks, even though there is an exact kink solution available theoretically. We therefore examined several possible definitions, all of which rely on a knowledge of the

canonical kink size. From the classical solution for a kink centered at x_0, $\phi=\tanh[(x-x_0)/\sqrt{2}]$, the kink scale L_k is approximately 8 lattice units. Raw kink configurations are shown in Fig. 1. At low enough temperatures ($\bar{\beta}>5$), kinks may be identified easily, however at higher temperatures this is clearly not the case.

The naive approach is to simply count the number of zero crossings of the field, since one may argue that these are the "tunneling events" which correspond to kinks. However, at higher temperatures there are zero crossings due to thermal noise (phonons), and counting all zero crossings would lead to a gross overestimation of the number of kinks. At high temperatures it is not possible to distinguish unambiguously between kinks and nonlinear phonons. However, the problem of the possible overcounting arises already at intermediate temperatures, where kinks are distinct. A possible solution is to use a smoothed field by either averaging or "block spinning" the actual field configuration over a length of the order of the kink length scale. The latter approach was taken in previous simulations [12–15]. This solution is not without flaws either, as rapid fluctuations can still appear as kinks. We prefer to count kinks in the following way: at a particular time we first find all zero crossings. To test the legitimacy of a given zero crossing we check for zero crossings one kink scale (8 lattice units) to its right and to its left. If no zero crossings are found, we count it as a kink, otherwise not.

The number of kinks is plotted against $\bar{\beta}$ in Fig. 2. Above $\bar{\beta}\sim 6$, the averaged field method and our method for counting kinks agree. Moreover, in this (low-temperature) range, the dilute gas expression for the kink number (11) is in excellent agreement with the data. At elevated temperatures, there is a clear disagreement between the two methods of counting kinks. The average field technique has the number of kinks monotonically increasing with temperature; whereas, in accord with intuition and the behavior of $P[\phi]$, the second technique
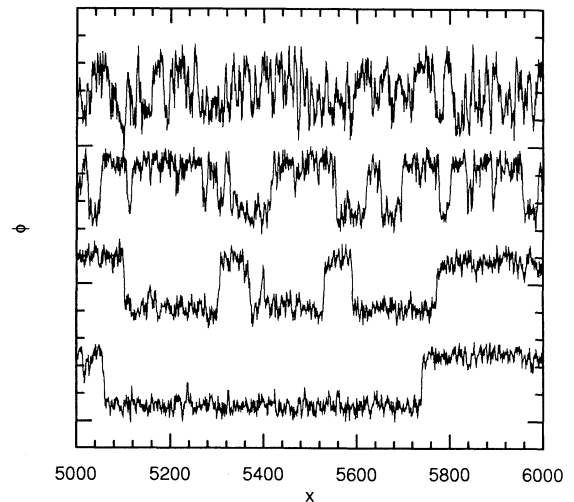

FIG. 1. Sample field configurations, from top to bottom, at $\bar{\beta}=2$, $\bar{\beta}=4$, $\bar{\beta}=5.5$, and $\bar{\beta}=8$. Only a 1000 lattice unit sample of the total lattice size of 16 384 is shown.
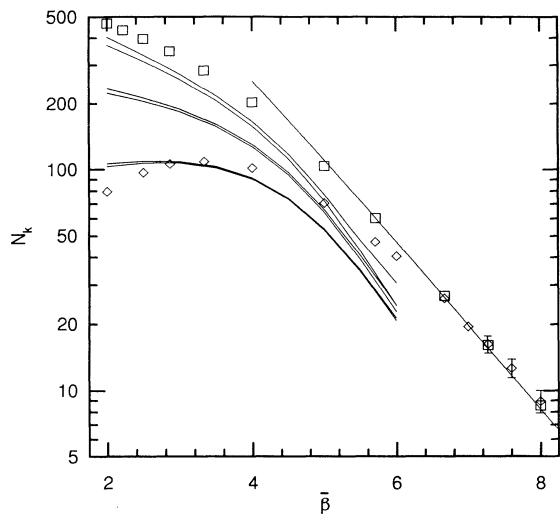
FIG. 2. Total number of kinks as a function of $\bar{\beta}$. Squares denote counts with a smoothed field ($l_a = 8$ lattice units) definition of kinks, diamonds for the zero-crossing counting method discussed in Sec. II, and the solid line starting at $\bar{\beta} = 4$ is a fit to the WKB prediction (11). Also shown are three predictions (the three pairs of solid lines) for the kink number from the theoretical formula (42) calculated in double-Gaussian approximation. Three values for the averaging length were used, from top to bottom, $l_a = 2$, 4, and 8 lattice units. For each value of l_a, there are two theoretical curves: (1) calculating (42) keeping only the ground and first excited states and (2) keeping the ground, and first and second excited states (the upper curves of each pair). The kink number is seen to strongly depend on l_a for $\bar{\beta} < 6$. (The double-Gaussian approximation breaks down at higher values of $\bar{\beta}$.)

FIG. 3. Field correlation length λ as a function of $\bar{\beta}$. The double-Gaussian (top curve) and WKB (bottom curve) predictions are compared with the numerical results. Squares are data points from the simulations. The crossover from the double-Gaussian to the WKB range of validity happens around $\bar{\beta} \sim 5$.

clearly shows a reduction in the kink number at higher temperatures (see Sec. IV for a detailed discussion). Moreover, in this temperature regime the number of kinks computed with the smoothing method depends strongly on the smoothing scale. We conclude that for $\bar{\beta} < 6$, an unambiguous number of kinks cannot be extracted with any confidence from the smoothing method. Unfortunately, this is precisely the temperature regime explored in previous simulations. We will discuss an analytic definition of the kink number N_k in Sec. III and show that this quantity can be independent of the smoothing scale only at low temperatures.

The correlation length was extracted from the field configurations by taking the inverse Fourier transform of the power spectrum and then fitting an exponential decay to the correlation function. The correlation length λ is plotted against $\bar{\beta}$ in Fig. 3. The WKB prediction is seen to hold for $\bar{\beta} > 6$ while at higher temperatures ($\bar{\beta} < 4$), the double Gaussian approximation is in excellent agreement with the data.

Our numerical results can be understood by using different analytical approaches in different temperature regimes. At low temperatures ($\bar{\beta} > 6$) the WKB method turns out to be very accurate. At higher temperatures a double Gaussian variational method provides a good description of our data. Both analytical methods are con-
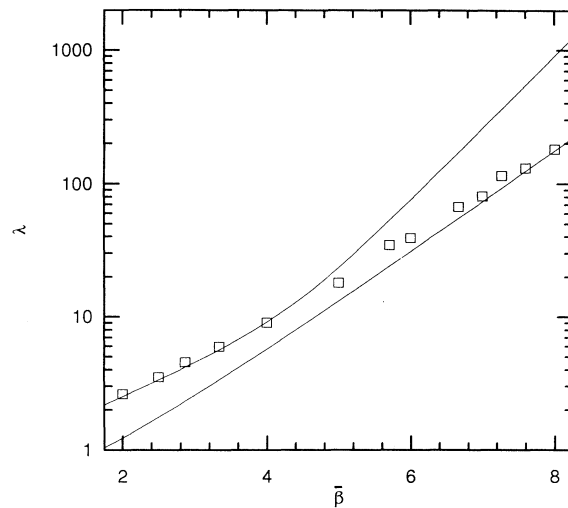
veniently discussed in the framework of the transfer-operator formalism, which we describe in the following section.

III. THE TRANSFER OPERATOR

The key idea behind the transfer-operator method is to transform the problem of finding the canonical partition function for a system to the exactly equivalent problem of finding the eigenvalues of a certain integral operator. With some smoothness assumptions for the eigenfunctions of this transfer operator, it is then possible to show that the problem reduces to that of finding the energy eigenvalues of a related quantum-mechanical problem. The method easily generalizes to the problem of calculating correlation functions. The presentation given here closely follows that of Ref. [10].

The canonical partition function for the Lagrangian (1) is given by the functional integral

$$Z = \int D\Phi \, D\pi \exp(-\beta H[\Phi, \pi]) , \qquad (17)$$

where π is the canonical momentum of the field and H is the field Hamiltonian. The integral over the momenta is a trivial Gaussian integral. Writing

$$Z = Z_\pi Z_\Phi , \qquad (18)$$

we have

$$Z_\pi = \left[\frac{2\pi}{\delta\beta} \right]^{N/2} \qquad (19)$$

obtained by discretizing the spatial lattice with lattice spacing δ. Periodic boundary conditions are assumed and the total lattice size $L = N\delta$. We will be primarily interested in obtaining the configurational partition func-

tion Z_Φ. Skeletonizing the formal path integral for Z_Φ by first forming

$$f(\Phi_{i+1},\Phi_i) = -\tfrac{1}{2}m^2\Phi_{i+1}^2 + \tfrac{1}{4}\Lambda\Phi_{i+1}^4 + \tfrac{1}{2}\left[\frac{\Phi_{i+1}-\Phi_i}{\delta}\right]^2$$

(20)

we have

$$Z_\Phi = \prod_{i=1}^{N} \int d\overline{\Phi}_i \exp[-\beta\delta f(\Phi_{i+1},\Phi_i)] ,$$

(21)

where as just stated we have imposed a periodic boundary condition ($\Phi_1 = \Phi_{N+1}$), and

$$d\overline{\Phi}_i = (\beta/2\pi\delta)d\Phi_i .$$

(22)

The normalization (22) is fixed by requiring equipartition to hold for a free scalar field theory.

Introducing the transfer operator specified by the eigenvalue problem,

$$\int d\overline{\Phi}_i \exp[-\beta\delta f(\Phi_{i+1},\Phi_i)]\Psi_n(\Phi_i)$$
$$= \exp(-\beta\delta\epsilon_n)\Psi_n(\Phi_{i+1}) ,$$

(23)

where ϵ_n is the eigenvalue corresponding to the eigenfunction Ψ_n. Substituting in (21), it follows from the completeness of the eigenfunctions that

$$Z_\Phi = \sum_n e^{-\beta L\epsilon_n} .$$

(24)

In the thermodynamic limit, $L \to \infty$, Z_Φ is determined by the smallest eigenvalue of the transfer operator. In this limit, the free-energy density is simply $F_\Phi = \epsilon_0$.

In an entirely analogous manner, it is possible to show that the correlation function

$$\langle \Phi(x)\Phi(0)\rangle = \frac{1}{Z_\Phi} \int D\overline{\Phi} e^{-\beta H[\Phi]}\Phi(x)\Phi(0)$$
$$= \sum_n |\langle\Psi_n|\Phi|\Psi_0\rangle|^2 \exp(-\beta|x|\Delta_{0n}) ,$$

(25)

where $\Delta_{0n} = \epsilon_n - \epsilon_0$. At large values of x, the lowest excited state controls the behavior of the correlation function.

The problem is now to compute the eigenvalues and eigenfunctions of the transfer operator. Assuming that $\Psi_n(\Phi_i)$ are smooth functions of Φ_i, we Taylor expand $\Psi_n(\Phi_i)$ on the left-hand side of (23) in terms of the $\Psi_n(\Phi_{i+1})$ on the right-hand side. The integral on the left-hand side can now be evaluated term by term. To leading order in δ/β, (23) becomes

$$\exp(-\beta\delta H_Q)\Psi_n = \exp(-\beta\delta\epsilon_n)\Psi_n$$

(26)

which is equivalent to the time independent Schrödinger equation

$$H_Q\Psi_n = \epsilon_n\Psi_n .$$

(27)

Dropping the indices on the fields

$$H_Q = -\frac{1}{2\beta^2}\frac{\partial^2}{\partial\Phi^2} - \tfrac{1}{2}m^2\Phi^2 + \tfrac{1}{4}\Lambda\Phi^4 + V_Q$$

(28)

is the quantum Hamiltonian for a particle in a double-well potential with a temperature-dependent energy shift

$$V_Q = \frac{1}{2\beta\delta}\ln\left[\frac{\beta}{2\pi\delta}\right]$$

(29)

arising from the normalization (22). The role of $\hbar$ is now played by β^{-1}, so that as the inverse temperature is made larger, WKB becomes a better approximation. For the dimensionless form of the theory (7), the quantum Hamiltonian (28) becomes

$$\overline{H}_Q = -\frac{1}{2\bar{\beta}^2}\frac{\partial^2}{\partial\phi^2} - \tfrac{1}{2}\phi^2 + \tfrac{1}{4}\phi^4 + \overline{V}_Q ,$$

(30)

where $\overline{V}_Q$ is just V_Q with β replaced by $\bar{\beta}$. This is the form of the theory that we will use in the remainder of the paper.

It is important to note that since (27) was derived under certain smoothness requirements, the eigenfunctions of H_Q or of $\overline{H}_Q$ will not always be eigenfunctions of the transfer operator. This is the case at high temperatures where, for fixed δ, the ratio δ/β may be much larger than unity. However, for the intermediate- and low-temperature regimes which are of relevance to kink thermodynamics, (27) provides an adequate description. (If needed, the high-temperature behavior can be studied via perturbation theory [20].)

An alternative way to view (30) is to introduce the scaled field $\bar{\phi} = \bar{\beta}\phi$, in which case,

$$\overline{H}_Q = \tfrac{1}{2}\bar{p}^2 - \frac{1}{2\bar{\beta}^2}\bar{\phi}^2 + \frac{1}{4\bar{\beta}^4}\bar{\phi}^4 .$$

(31)

Here we have omitted the contribution of $\overline{V}_Q$ which, since it is just a shift, can be treated separately.

At low temperatures the two wells are widely separated and the ground-state energy is given by the oscillator ground-state energy for one of the wells minus the tunnel-splitting term, usually calculated by the WKB method. One can then write

$$Z_\phi = Z_{\text{osc}}Z_{\text{tunn}}Z_{\overline{V}_Q}$$

(32)

or, in terms of the free energies,

$$F = F_{\text{osc}} + F_{\text{tunn}} + \overline{V}_Q ,$$

(33)

where, from a crude WKB estimate,

$$F_{\text{osc}} \sim \frac{L}{\sqrt{2}\bar{\beta}}$$

(34)

and

$$F_{\text{tunn}} \sim -\frac{L}{2\sqrt{2}\bar{\beta}}e^{-\overline{E}_k\bar{\beta}} ,$$

(35)

where the kink energy for the dimensionless form of the theory, $\overline{E}_k = \sqrt{8}/9$. The key result of KS is the realization that the tunneling contribution is associated with kinks and the sum of all the other contributions with phonons [8].

More generally, one expects that there should be three qualitatively distinct temperature ranges. At very low temperatures the tunnel splitting between two "classically

degenerate" states is very small and the WKB picture of kinks is valid. At higher temperatures the wave-function overlap in the region between the wells is large enough that the WKB result for the energy difference between the ground and first excited state is incorrect. One expects, therefore, that for temperatures in this "intermediate overlap" regime, the WKB approximation breaks down, but that kinks still exist as fairly well identifiable objects. Moreover, the tunnel splitting between the ground states can become comparable to the splitting between a ground state and the first excited state inside each well (this, however, has no effect on the correlation length, and as seen in Fig. 2, makes only a minor correction to the kink number). Finally, at still higher temperatures when the ground-state energy in each well becomes larger than the classical barrier height, the kink description fails since the overlap is of order unity and the kink and phonon energy scales become indistinguishable. These three temperature regimes are in fact clearly seen in our numerical data (Fig. 1) as well as in the analytic results from the double-Gaussian approximation of Sec. IV (Fig. 5).

Let us first describe the expectation values for the correlator and the kink density based on the WKB approximation, which one expects to be valid in the low-temperature regime. [From now on we perform all calculations in the thermodynamic limit $L \to \infty$. The large size of the system in our simulation (16384 sites) rules out finite-size effects: from (24), it is clear that the thermodynamic limit is correctly found in the simulation provided that $L\Delta_{01}\bar{\beta} \gg 1$, or in terms of the correlation length, when $L \gg \lambda$. At the lowest temperature studied here $L/\lambda > 40$. Since this is the worst case result, the condition $L \gg \lambda$ is very well satisfied over the full range of the simulation.] An accurate calculation in this limit (see, e.g., Ref. [9]) yields, for the energy difference between the ground and first excited state,

$$\Delta_{01} = 4 \left[\frac{3\bar{E}_k}{\bar{\beta}\pi} \right]^{1/2} \exp(-\bar{E}_k\bar{\beta}) . \tag{36}$$

The WKB result for the correlation function (using only the first two states) is

$$\langle \phi(0)\phi(x) \rangle \simeq e^{-|x|/\lambda} , \tag{37}$$

where the correlation length

$$\lambda = \frac{1}{\bar{\beta}\Delta_{01}} \tag{38}$$

$$= \frac{1}{4}\sqrt{(\pi/3)} \frac{1}{\sqrt{\bar{E}_k\bar{\beta}}} \exp(\bar{E}_k\bar{\beta}) . \tag{39}$$

This is plotted in Fig. 3 and is seen to fit the numerical data very well for $\bar{\beta} > 6$.

Another quantity of interest is the number of kinks. In fact, there appears to be no unambiguous way to define this quantity. The number of kinks is usually calculated in the phenomenological approach by working in the grand canonical ensemble (see, e.g., Ref. [9]). We now introduce a new way of defining an effective kink number by working only with the original field variable. We be-

gin by identifying three length scales in the problem: l_a, the averaging scale, a length scale long enough such that the averaged field

$$\phi_a(\bar{x}) = \frac{1}{l_a} \int_{-l_a/2}^{l_a/2} d\bar{y} \, \phi(\bar{x}+\bar{y}) \tag{40}$$

is smooth on scales of the order of the kink length. Calling the typical kink separation, l_k, and with L_s such that $l_a \leq L_s \ll l_k$, we define

$$N_k = \frac{1}{2}\left\langle \frac{(\phi_a(0)-\phi_a(L_s))^2}{4\phi_0^2} \right\rangle$$

$$= \frac{1}{4\phi_0^2}[\langle \phi_0^2 \rangle - \langle \phi_a(0)\phi_a(L_s) \rangle] \tag{41}$$

to be the kink number density. This definition comes from just counting the number of zero crossings of the smoothed field under an assumption that the typical separation between the kinks is much larger than l_a and L_s. The normalization factor $\pm\phi_0$ is the asymptotic field value away from a kink. The angular brackets denote a sampling over the whole lattice (divided into blocks of length L_s). The factor $\frac{1}{2}$ compensates for the fact that antikinks are also counted (the number of kinks is equal to the number of antikinks). Note that our definition of kink number is sensible only when there is an appropriate separation of length scales, e.g., it is not valid at high temperatures when the kink separation is very small (where even the notion of a kink is not well defined). Even at intermediate temperatures, N_k depends on the smearing length. Such a dependence has indeed been noted in numerical simulations [15,19].

To understand the errors in estimating the number of kinks from (41) we first consider the case of l_a fixed and varying L_s. If, on the one hand, L_s is chosen too large $(L_s > l_k)$ then there is an undercounting of the total number of kinks since there will be many instances of having more than one kink in a block of length L_s. If, on the other hand, L_s is too small (i.e., smaller than the kink size) then there will again be an undercounting since in any given block of size L_s, $|\phi_a(0)-\phi_a(L_s)| < 2\phi_0$. Therefore, for a given l_a, one should maximize (41) with respect to L_s. Now, considering l_a as a variable, it is clear that for small l_a (l_a less than the kink size), (41) can be nonzero as long as non-negligible phonon fluctuations are present *independent* of whether kinks exist or not. At low temperatures one expects N_k to be independent of l_a (see the discussion below) but in the intermediate-temperature regime there should be a dependence on the averaging scale.

An explicit formula for N_k can be obtained by substituting (40) in (25). Then, for $L_s \geq l_a$, it is easy to show that

$$N_k = \frac{1}{2\phi_0^2\bar{\beta}^2 l_a^2} \sum_n \frac{|\langle 0|\phi|n \rangle|^2}{\Delta_{0n}^2} \{ \bar{\beta}\Delta_{0n}l_a - 1 + e^{-\bar{\beta}l_a\Delta_{0n}}$$

$$+ e^{-\bar{\beta}L_s\Delta_{0n}}$$

$$\times [1-\cosh(\bar{\beta}\Delta_{0n}l_a)]\} . \tag{42}$$

In the dilute-gas regime we keep only the contribution of the first excited state in (42), use the WKB result (36) for Δ_{01}, and take the limit $\beta \to \infty$ in (42). The total number of kinks is, for $L_s \geq l_a$,

$$N_{\text{tot}} \simeq \frac{L}{L_s} L_s \left[1 - \frac{l_a}{3L_s} \right] \sqrt{(3/\pi)} \sqrt{\bar{E}_k \bar{\beta}_e} e^{-\bar{E}_k \bar{\beta}}$$

$$= L \left[1 - \frac{l_a}{3L_s} \right] \sqrt{(3/\pi)} \sqrt{\bar{E}_k \bar{\beta}} e^{-\bar{E}_k \bar{\beta}} , \quad (43)$$

which, modulo the constant prefactor, is in agreement with the result of Ref. [9] in this limit. An interesting point is that we have an explicit expression for the prefactor and therefore can test our formula directly against the simulations.

Our predictions are compared with results from the simulations in Fig. 2. (Note that the kink energy in the dimensionless form of the theory $\bar{E}_k = \sqrt{8/9}$ and that $\bar{E}_k \bar{\beta} = E_k \beta$.) In the low-temperature limit, one expects the kink number to be independent of L_s, and this is indeed true provided that $l_a \ll L_s$ [see (43)]. In this case, while the analytic result overestimates the number of kinks by a multiplicative factor of ~ 1.6, the functional form of the temperature dependence of the kink number is in very good agreement with the simulations. If one sets $L_s = l_a$ in (43) then compared with the previous case, the kink number is reduced by a factor of $\frac{2}{3}$, and is in complete agreement with the simulations. At present we do not understand the sensitivity of the theoretical formula to the ratio of l_a/L_s in the low-temperature regime. A discussion of the kink number density in the intermediate temperature regime will be postponed to Sec. IV, after we have described the double-Gaussian approximation.

The agreement of the WKB or dilute-gas results with the simulations imply that there is no significant renormalization of the kink energy (beyond that due to linearized phonons) at low temperatures (i.e., $\beta > 6$). This is in disagreement with the simulations carried out in Ref. [11] but in agreement with the theory of Ref. [9]. Whether there is or not such a renormalization of the kink mass at intermediate temperatures is difficult to analyze as at these temperatures the effects due to nonlinear phonons and kinks are hard to disentangle. A good example of this is the behavior of the kink number versus $\bar{\beta}$ (Fig. 2). Both numerical and analytic results show that the ambiguity in the very notion of a kink number density is such as to rule out any estimation of the kink mass from the data at intermediate temperatures.

In the regime where WKB fails, one can compare the simulations of the kink system with numerical solutions for the energy eigenvalues of the Hamiltonian $\bar{H}_Q$. However, one would like to have a simple analytical method for predicting the measured quantities. To this end we implement the double-Gaussian variational approximation in the effective quantum-mechanical problem. This approximation is an order of magnitude more accurate than the simple Gaussian approximation for this problem and correctly accounts for the reduction of energy due to the overlap between the wave functions in the two wells. It also allows a natural decomposition of phonon and

kink contributions in terms of separate "diagonal" and "overlap" contributions to the ground-state energy. The double-Gaussian approximation should be reliable at intermediate and high temperatures, where the overlap between the two ground states is substantial (at low temperatures, when the overlap is very sensitive to the form of the "tail" of the wave function, WKB is more accurate).

IV. THE DOUBLE-GAUSSIAN APPROXIMATION

The Gaussian approximation is a well-known nonperturbative variational method for calculating the ground-state energy and effective potentials in quantum-mechanics and quantum-field theory [22]. As discussed in the previous section, the transfer-operator technique reduces the classical statistical mechanics of a field theory in $1+1$ dimensions to ordinary quantum mechanics. To apply the standard Gaussian approximation is simple: one assumes that the ground-state wave function is a Gaussian with width $\Omega^{-1/2}$, and centered at the point $\bar{\phi}_0$,

$$\Psi_G(\bar{\phi}_0, \Omega) = \sqrt{(\Omega/\pi)} \exp[-\tfrac{1}{2}\Omega(\bar{\phi} - \bar{\phi}_0)^2] . \quad (44)$$

Next one computes the energy

$$V_G(\bar{\phi}_0, \Omega) \equiv \langle \Psi_G | H_Q | \Psi_G \rangle , \quad (45)$$

and minimizes with respect to Ω to yield the Gaussian effective potential $V_G(\bar{\phi}_0)$. The global minimum of $V_G(\bar{\phi}_0)$ is the ground-state energy as calculated in the Gaussian approximation.

In our case, with the Hamiltonian given by (31), it is easy to show that

$$V_G(\bar{\phi}_0, \Omega) = \tfrac{1}{4}\Omega - \frac{1}{2\bar{\beta}^2} \left[\bar{\phi}_0^2 + \frac{1}{2\Omega} \right]$$
$$+ \frac{1}{4\bar{\beta}^4} \left[\bar{\phi}_0^4 + \frac{3}{4\Omega^2} + \frac{3\bar{\phi}_0^2}{\Omega} \right] . \quad (46)$$

Minimization of (46) with respect to Ω yields the cubic equation

$$\Omega^3 + \frac{\Omega}{\bar{\beta}^2} \left[1 - \frac{3}{\bar{\beta}^2}\bar{\phi}_0^2 \right] - \frac{3}{2\bar{\beta}^4} = 0 , \quad (47)$$

the largest positive root of which is of interest. Substitution of (47) in (46) enables us to write

$$V_G(\bar{\phi}_0) = -\frac{1}{2\bar{\beta}^2}\bar{\phi}_0^2 + \frac{1}{4\bar{\beta}^4}\bar{\phi}_0^4 + \tfrac{1}{2}\Omega - \frac{3}{16\bar{\beta}^4}\frac{1}{\Omega^2} . \quad (48)$$

Note that $\bar{\phi}_0 = 0$ is always a local minimum of $V_G(\bar{\phi}_0)$. Above a certain temperature, it becomes the global minimum and one has a behavior reminiscent of a first-order phase transition in the effective potential (Fig. 4). Numerically, this transition occurs at $\bar{\beta} = 3.12$ and one might interpret this as predicting a disappearance of kinks at this temperature. This is not quite correct, however, as we will soon see.

A problem with the Gaussian approximation is that it does not account for tunneling. We know intuitively that for the double-well Hamiltonian, at large well separation, the ground state should be described by a superposition
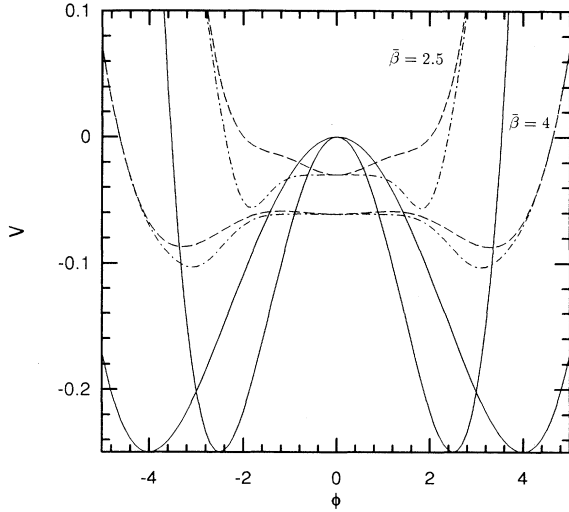
FIG. 4. The Gaussian effective potential V_G (dashed lines) compared with V_{DG} (dot-dashed lines) at the two temperatures ($\bar{\beta}=2.5$ and 4). The classical potential $V=-[1-\bar{\phi}^2/(2\bar{\beta}^2)]\bar{\phi}^2/(2\bar{\beta}^2)$ from (31) is also shown (solid curves). For $\bar{\beta}<3.12$, V_G has a global minimum at the origin, while for $\bar{\beta}<3.12$ there are two degenerate global minima. For V_{DG} the origin is always a maximum and there are always two degenerate minima. The ground-state energy calculated in the two approximations is the global minimum of V_G or of V_{DG}. The ground-state energy is always lower in the double-Gaussian approximation.

of two localized wave packets, one in each well. These wave packets may be taken to be Gaussians. With such a wave function there will be cross terms in $\langle \Psi|H_Q|\Psi \rangle$ arising from overlaps between the individual Gaussians. Correctly accounting for these overlap terms is clearly essential for our problem.

We therefore modify the trial wave function by taking it as a superposition of two Gaussians,

$$\Psi_{DG}=\frac{1}{N}[\Psi_G(\bar{\phi}_0,\Omega)+\Psi_G(-\bar{\phi}_0,\Omega)] \ , \tag{49}$$

where the normalization factor

$$N^2=2[1+e^{-\Omega\bar{\phi}_0^2}] \ . \tag{50}$$

It is then a simple matter to show that

$$V_{DG}(\bar{\phi}_0,\Omega)=\langle \Psi_{DG}|\bar{H}_Q|\Psi_{DG} \rangle$$

$$=\frac{2}{N^2}\left[V_G(\bar{\phi}_0,\Omega)\right.$$

$$\left.+e^{-\Omega\bar{\phi}_0^2}\left[-\frac{\Omega^2\bar{\phi}_0^2}{2}-\frac{1}{4\bar{\beta}^2\Omega}+\frac{3}{16\bar{\beta}^4\Omega^2}\right.\right.$$

$$\left.\left.+\frac{\Omega}{4}\right]\right] . \tag{51}$$

The first term represents the "diagonal" contribution to the energy while the rest are cross terms from the overlap or "off-diagonal" contribution. In the framework of the

phonon-kink model these terms have a natural interpretation: the diagonal term corresponds to a contribution to the free energy due to phonons (including anharmonic corrections) while the overlap term is the kink contribution. In the low-temperature limit this reproduces the WKB splitting of the free energy into phonons and kinks.

In principle, one can minimize V_{DG} by following the same procedure as for V_G. Unfortunately, this yields a transcendental equation for Ω which cannot be handled analytically. A way out is to first minimize (51) with respect to Ω ignoring the overlap terms completely: this amounts to keeping Ω as given by (47) in (51). The minimization with respect to $\bar{\phi}_0$ is then carried out by differentiating (51) with respect to $\bar{\phi}_0$ and setting the result to zero. While this procedure appears to be rather a drastic simplification, it is still a major improvement over V_G both qualitatively and quantitatively. First, $V_{DG}(\bar{\phi}_0)$ always has a local maximum at $\bar{\phi}_0=0$ so that there is no abrupt change in the behavior of $V_{DG}(\bar{\phi}_0)$ with temperature, consistent with the fact that there is no finite temperature phase transition in this model (V_{DG} and V_G are compared in Fig. 4). Second, it is an order of magnitude more accurate than V_G in estimating the ground-state energy (worst case error $\sim 1\%$ compared to $\sim 15\%$). Third, and very importantly, we can now estimate the energy of the higher excited states.

To estimate the energy of the first excited state we simply minimize $V_{DG}^{(1)}\equiv\langle \Psi_1|H_Q|\Psi_1 \rangle$ where Ψ_1 is the antisymmetric partner of Ψ_{DG},

$$\Psi_1=\frac{1}{\bar{N}}[\Psi_G(\bar{\phi}_1,\Omega_1)-\Psi_G(-\bar{\phi}_1,\Omega_1)] \tag{52}$$

with $\bar{N}^2=2[1-\exp(-\Omega_1\bar{\phi}_1^2)]$. It is to be stressed that the minimization of the energy with respect to Ψ_1 has to be done independently from that with Ψ_{DG}. We find that

$$V_{DG}^{(1)}(\bar{\phi}_1,\Omega_1)=\frac{2}{\bar{N}^2}\left[V_G(\bar{\phi}_1,\Omega_1)\right.$$

$$\left.-e^{-\Omega_1\bar{\phi}_1^2}\left[-\frac{\Omega_1^2\bar{\phi}_1^2}{2}-\frac{1}{4\bar{\beta}^2\Omega_1}\right.\right.$$

$$\left.\left.+\frac{3}{16\bar{\beta}^4\Omega_1^2}+\frac{\Omega_1}{4}\right]\right] . \tag{53}$$

The difference between the absolute minima of $V_{DG}^{(1)}$ and V_{DG} is the tunnel-splitting energy Δ_{01} calculated in the double-Gaussian approximation. We now investigate the low-temperature limit of the double-Gaussian approximation and contrast it with the WKB result. First, from (47), it follows immediately that at low temperatures,

$$\Omega\simeq\frac{\sqrt{2}}{\bar{\beta}} \ . \tag{54}$$

Also, at low temperatures, $\bar{\phi}_0\simeq\bar{\beta}$. Substituting these last two results in (51) and (53) we find,

$$V_{DG} \simeq \frac{1}{\sqrt{2}\bar{\beta}} + \frac{3}{32\bar{\beta}^2} - \frac{1}{4} - \frac{e^{-\sqrt{2}\bar{\beta}}}{4}\left[4 - \frac{1}{\sqrt{2}\bar{\beta}} - \frac{3}{8\bar{\beta}^2}\right],$$
$$\bar{\beta} \to \infty \quad (55)$$

and

$$V_{DG}^{(1)} \simeq \frac{1}{\sqrt{2}\bar{\beta}} + \frac{3}{32\bar{\beta}^2} - \frac{1}{4} + \frac{e^{-\sqrt{2}\bar{\beta}}}{4}\left[4 - \frac{1}{\sqrt{2}\bar{\beta}} - \frac{3}{8\bar{\beta}^2}\right],$$
$$\bar{\beta} \to \infty . \quad (56)$$

Polynomial corrections in powers of $\bar{\beta}^{-1}$ to the leading order result are due to anharmonic corrections while the exponential terms represent the tunneling contribution. On subtracting (55) from (56) the tunnel-splitting term follows immediately:

$$\Delta_{01} \simeq \frac{e^{-\sqrt{2}\bar{\beta}}}{2}\left[4 - \frac{1}{\sqrt{2}\bar{\beta}} - \frac{3}{8\bar{\beta}^2}\right], \quad \bar{\beta} \to \infty , \quad (57)$$

which may be contrasted with the WKB result (36). In this regime, the WKB result is more accurate as the double-Gaussian method tends to underestimate the overlap contribution [$\Delta_{01} \sim \exp(-\sqrt{2}\bar{\beta})$ in double Gaussian versus $\Delta_{01} \sim \exp(-\sqrt{8/9}\bar{\beta})$ in WKB]. This is to be expected since in this regime the overlap between the two

wave packets is very small and therefore very sensitive to the form of the tail of the wave function. At higher temperatures, however, the overlap is not small and the sensitivity to the form of the tail disappears. Consequently, (51) and (53) become increasingly more accurate.

At low temperatures, the second excited state is one of a pair of tunnel-split harmonic-oscillator first excited states. The state with even parity does not contribute to the correlation function or to the approximate kink number formula because the matrix element of the position operator between the ground state and any even state vanishes. The odd state, written in our double-Gaussian approximation is,

$$\Psi_2 = \frac{1}{\tilde{N}}[(\bar{\phi} - \bar{\phi}_2)\Psi_G(\bar{\phi}_2, \Omega_2) + (\bar{\phi} + \bar{\phi}_2)\Psi_G(-\bar{\phi}_2, \Omega_2)] , \quad (58)$$

and

$$\tilde{N}^2 = \frac{1}{\Omega_2} + e^{-\Omega_2\bar{\phi}_2^2}\left[\frac{1}{\Omega_2} - 2\bar{\phi}_2^2\right] . \quad (59)$$

The expectation value of the energy in this state now follows from a straightforward calculation:

$$V_{DG}^{(2)} \equiv \langle \Psi_2 | H_Q | \Psi_2 \rangle$$
$$= \frac{3}{4\tilde{N}^2}\left[1 - \frac{1}{\bar{\beta}^2\Omega_2^2}(1 + \tfrac{2}{3}\Omega_2\bar{\phi}_2^2) + \frac{1}{\bar{\beta}^4\Omega_2^3}(\tfrac{5}{4} + 3\Omega_2\bar{\phi}_2^2 + \tfrac{1}{3}\Omega_2^2\bar{\phi}_2^4)\right.$$
$$\left. + e^{-\Omega_2\bar{\phi}_2^2}\left\{1 - 4\Omega_2\bar{\phi}_2^2 + \tfrac{4}{3}\Omega_2^2\bar{\phi}_2^4 - \frac{1}{\bar{\beta}^2\Omega_2^2}(1 - \tfrac{2}{3}\Omega_2\bar{\phi}_2^2) + \frac{1}{\bar{\beta}^4\Omega_2^3}(\tfrac{5}{4} - \tfrac{1}{2}\Omega_2\bar{\phi}_2^2)\right\}\right] . \quad (60)$$

In order to determine the values of $\bar{\phi}_2$ and Ω_2 one has, in principle, to carry out a constrained minimization of the energy by also enforcing the requirement that Ψ_1 and Ψ_2 be orthogonal. From (52) and (58) this condition turns out to be

$$\frac{\bar{\phi}_2 - \bar{\phi}_1}{\bar{\phi}_2 + \bar{\phi}_1} = \exp\left[-\frac{2\Omega_1\Omega_2}{\Omega_1 + \Omega_2}\bar{\phi}_1\bar{\phi}_2\right] . \quad (61)$$

For the range of temperatures we are interested in, the above condition is reasonably well satisfied if we take $\Omega_1 = \Omega_2$ and $\bar{\phi}_1 = \bar{\phi}_2$, i.e., the left-hand side of (61) is identically zero, while the right-hand side is small (worst case of order 10^{-2}). Therefore for this state we do not need to carry out a minimization of the energy as long as high accuracy is not required. In the low-temperature limit,

$$V_{DG}^{(2)} \simeq \frac{3}{\sqrt{2}\bar{\beta}} + \frac{15}{32\bar{\beta}^2} - \tfrac{1}{4} + O(e^{-\sqrt{2}\bar{\beta}}), \quad \bar{\beta} \to \infty . \quad (62)$$

The first term in (62) is just the energy of the first excited harmonic-oscillator state as expected. The other terms represent anharmonic corrections and overlap contributions as usual. In Fig. 5, the first three energies (as calculated in double-Gaussian approximation) are plotted
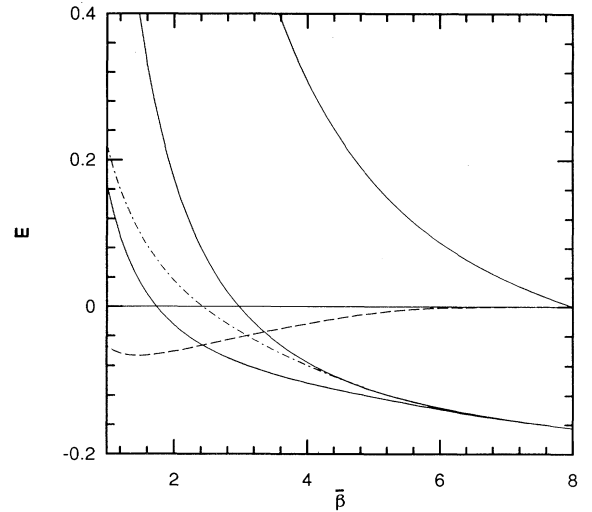

FIG. 5. The ground state, first excited, and the odd second excited state energies computed in the double-Gaussian approximation (the lowest, middle, and uppermost solid lines) plotted against $\bar{\beta}$. The ground-state energy has further been decomposed into the contributions from the "diagonal" (dot-dashed line) and "overlap" (dashed line) pieces.

against the inverse temperature. While at intermediate temperatures Δ_{02} and Δ_{01} are of similar magnitude, at low temperatures, $\Delta_{02} \gg \Delta_{01}$ which, of course, is just the WKB regime. It is clear that for values greater than $\bar{\beta} \sim 6$, the WKB results should hold.

The behavior of the energies of the ground and first two excited states (Fig. 5) allows the identification of three qualitatively different regimes: (1) all the energies lie above the classical barrier, (2) the ground-state energy lies below the classical barrier height (at $\bar{\beta} = 1.734$), and (3) the energy difference between the first two states becomes negligible in comparison with the energy difference between the ground and the second excited state (at $\bar{\beta} \sim 6$). Our simulations confirm the theoretical expectations of the previous section that kinks cannot be identified in region (1), that there are kinks, but that the dilute-gas approximation is invalid in region (2), and finally, that the dilute-gas approximation is accurate in region (3).

The classical single-point field distribution function $P(\bar{\phi})$ can be measured directly from our simulations. For the analogous quantum-mechanical problem arising from the transfer-operator method this is just the square of the ground-state wave function Ψ_0. Results from the simulations are compared with Ψ_{DG}^2 at $\bar{\beta} = 2$ and $\bar{\beta} = 4$ in Fig. 6 and are in reasonable agreement. The presence of kinks implies a double peak in $P(\bar{\phi})$ [23] (the converse is false) while a single peak centered at the origin means that kinks and large amplitude thermal phonons can no longer be distinguished. From the simulations such a transition occurs at $\bar{\beta} \simeq 1.7$, in agreement with the theoretical calculation of when Ψ_{DG}^2 goes over from a double- to single-peaked distribution. (The double-Gaussian method compares favorably with the numerical evaluation of the transfer operator in Ref. [20], which predicts $\bar{\beta} \simeq 1.8$ as
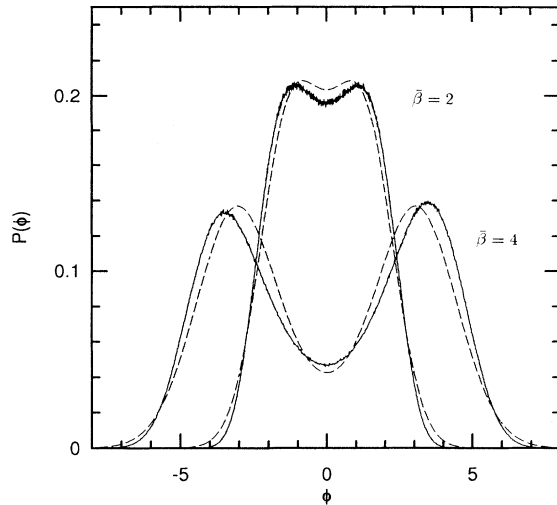

FIG. 6. The classical distribution function $P([\tilde{\phi}])$ (solid lines) given by the simulation and the distribution Ψ_0^2 from the double-Gaussian approximation (dashed lines) plotted against $\tilde{\phi}$ for $\bar{\beta} = 2$ and 4. The underestimation of the wave-function overlap in the double-Gaussian approximation is already visible at $\bar{\beta} = 4$.

the transition point.) As expected, this is also the temperature (see Fig. 2) where the ground-state energy crosses the classical barrier height. (A discussion of various methods to determine this characteristic temperature is given in Ref. [24].)

It is also apparent from Fig. 6 that the double peaks in the distribution function move inward from the minimum of the classical potential as the temperature increases (eventually coalescing at $\bar{\beta} \sim 1.7$). Physically this can be understood as nonlinear phonon corrections due to the fact that near each minimum, the potential is not symmetric under reflection around the minimum.

The correlation function as determined by (25) can, of course, be directly evaluated in the double-Gaussian approximation. The correlation length is determined by the long-distance behavior of the correlation function, and as is clear from (38), one needs only the energy difference between the ground and first excited state to determine the correlation length. In Fig. 3 the correlation length as given by the double-Gaussian and WKB approximations [see (13)] is compared with the results from the simulations. As expected, the double-Gaussian prediction is borne out at intermediate temperatures (up to $\bar{\beta} \sim 4$) whereas the WKB results are in agreement with the data at low temperatures (above $\bar{\beta} \sim 6$).

The kink number as determined by (42) requires the calculation of the matrix elements $\langle 0|\phi|n \rangle$. The first two nonzero matrix elements as given by the double-Gaussian approximation are

$$\langle 0|\bar{\phi}|1 \rangle = \Gamma \left[a_+ \exp\left[\frac{(\Omega\bar{\phi}_0 + \Omega_1\bar{\phi}_1)^2}{4\sigma} \right] \right.$$
$$\left. - a_- \exp\left[\frac{(\Omega\bar{\phi}_0 - \Omega_1\bar{\phi}_1)^2}{4\sigma} \right] \right] , \qquad (63)$$

$$\langle 0|\bar{\phi}|2 \rangle = \Gamma \left[\left[\frac{1}{2\sigma} + a_+^2 - a_+\bar{\phi}_1 \right] \exp\left[\frac{(\Omega\bar{\phi}_0 + \Omega_1\bar{\phi}_1)^2}{4\sigma} \right] \right.$$
$$+ \left[\frac{1}{2\sigma} + a_-^2 + a_-\bar{\phi}_1 \right]$$
$$\left. \times \exp\left[\frac{(\Omega\bar{\phi}_0 - \Omega_1\bar{\phi}_1)^2}{4\sigma} \right] \right] , \qquad (64)$$

where

$$\Gamma = \frac{2}{N\tilde{N}} \left[\frac{\Omega\Omega_1}{\sigma^2} \right]^{1/4} e^{-(1/2)(\Omega\bar{\phi}_0^2 + \Omega_1\bar{\phi}_1^2)} , \qquad (65)$$

$$\sigma = \tfrac{1}{2}(\Omega + \Omega_1) , \qquad (66)$$

$$a_\pm = \frac{\Omega\bar{\phi}_0 \pm \Omega_1\bar{\phi}_1}{\Omega + \Omega_1} . \qquad (67)$$

As the energies for the first three states are already known we can now evaluate the kink densities as given by (42). Theoretical estimates (for different choices of l_a and L_s) are compared with results from the simulation in Fig. 2. The double-Gaussian results for the kink density are entirely consistent with the numerical data at $\bar{\beta} < 5.5$

(beyond this temperature the double-Gaussian approximation underestimates the number of kinks due to the underestimation of Δ_{01}). Due to the ambiguity in the concept of kink number discussed earlier, the significance of this comparison at high temperatures is not clear.

The internal energy and the specific heat can be computed straightforwardly from the double-Gaussian approximation. The behavior of the specific heat with temperature is of particular interest: it is known that at a temperature relatively close to, but somewhat below the characteristic temperature where kinks appear, the specific heat attains a maximum value. Though a real phase transition cannot occur in this system, it can be argued that this peak is a signal for the emergence of a new degree of freedom, in this case presumably, the kinks. While this peak has been seen in numerical calculations of the partition function [20], it has not been unambiguously established that this feature is due to kinks. As remarked earlier, the ground-state energy as given by the double-Gaussian approximation breaks into two contributions: one given by an overlap contribution and arguably associated with kinks, the other associated with phonons. This feature allows one to analyze the nature of the peak in the specific heat.

To begin, we recall the definitions,

$$U = \frac{\partial}{\partial \bar{\beta}}(\bar{\beta}F) \tag{68}$$

and

$$C_v = -\bar{\beta}^2 \frac{\partial^2}{\partial \bar{\beta}^2}(\bar{\beta}F) \tag{69}$$

for the internal energy U and the specific heat C_v. In our case, the free energy F has four contributions: one from the kinetic term in the original field Hamiltonian, one from the term given by the normalization of the functional integral, one from the overlap contribution, and one from the (potentially nonlinear) oscillations around the potential minimum of $\bar{H}_Q$. The first contribution stems from (19) giving rise to the free energy density

$$F_\pi = -\frac{1}{\bar{\beta}L}\ln(Z_\pi)$$

$$= -\frac{1}{2\bar{\beta}\delta}\ln\left[\frac{2\pi}{\delta\bar{\beta}}\right]. \tag{70}$$

The other pieces come from (32). The contribution F_{osc} is just the first term of (51) while F_{tunn} is the second term. The normalization contributes the $\bar{V}_Q$ term. From (70) and (29) we can immediately calculate the contribution to the internal energy density and the specific heat (per unit length) of the kinetic and measure terms. This gives just the results for a free field theory

$$U_0 = \frac{1}{\delta\bar{\beta}}, \tag{71}$$

$$C_v^{(0)} = \frac{1}{\delta}. \tag{72}$$

Put another way, (71) and (72) are the contributions from

linear phonons. The nontrivial contributions are therefore included exclusively in F_{osc} and F_{tunn}. At low temperatures, the WKB result for the ground-state energy may be used to show that [9]

$$C_v^{(\phi)} \simeq 2\left[\frac{3E_k\bar{\beta}}{\pi}\right]^{1/2}[(\tfrac{1}{2}-E_k\bar{\beta})^2-\tfrac{1}{2}]e^{-E_k\bar{\beta}}, \quad \bar{\beta}\to\infty . \tag{73}$$

In this regime F_{osc} does not contribute to the specific heat at all while the kink contribution is exponentially suppressed. The constant term due to linear phonons (72) is dominant.

The situation can be dramatically different at intermediate temperatures. The specific heat as calculated from the double-Gaussian approximation is plotted in Fig. 7: A prominent peak in the specific heat appears at $\bar{\beta} \simeq 5.4$. To understand whether this peak is due to kinks, the individual contributions from F_{osc} and F_{tunn} are also plotted. There seems to be a delicate interplay between these two contributions. While the rise to the peak with increasing $\bar{\beta}$ is due to nonlinear phonons, just before the peak this contribution drops off steeply and eventually leads to a *reduction* in the height of the peak. The overlap or kink contribution exhibits a slow initial decline as $\bar{\beta}$ increases, followed by a relatively sharp peak: it is this peak that is the dominant contribution at $\bar{\beta} \sim 5.4$. We can therefore conclude that it is indeed the kinks that are responsible for the peak in the specific heat at this temperature. At larger values of $\bar{\beta}$, both contributions fall off smoothly to zero as expected from the low-temperature result (73).

We have also calculated the internal energy U. The nonlinear phonon and kink energies are plotted in Fig. 8.
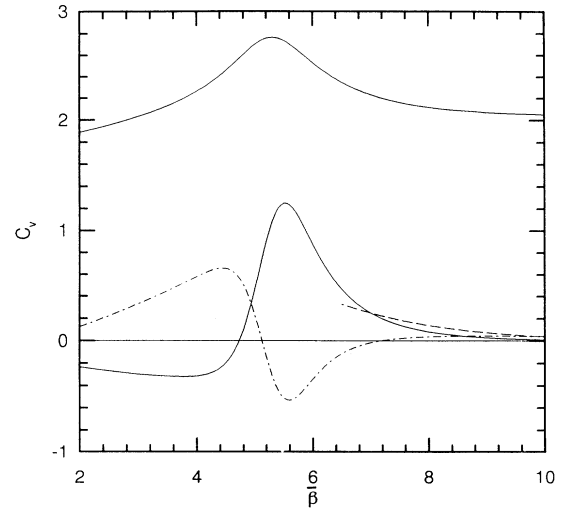
FIG. 7. The specific heat C_v as calculated from the double-Gaussian approximation plotted against $\bar{\beta}$ (top curve). The peak in the specific heat occurs at $\bar{\beta} \simeq 5.4$. The contribution of the linear phonons to the specific heat is the constant value $1/\delta = 2$. The individual contributions arising from the kinks (solid line) and nonlinear phonons (dot-dashed line) are shown below. The WKB calculation for the kink contribution (dashed line) is plotted from $\bar{\beta} = 6.5$ onwards.
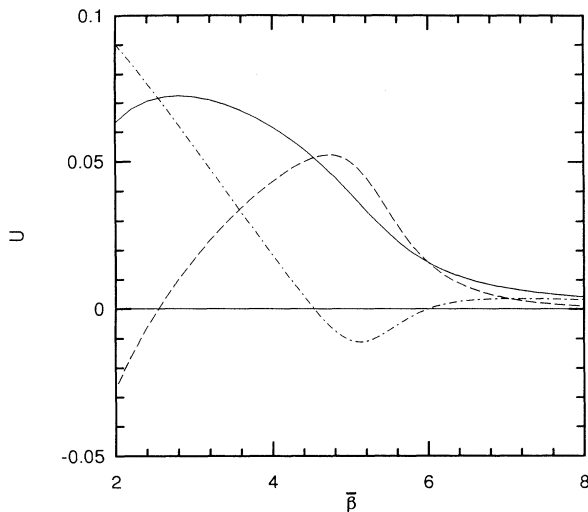
FIG. 8. The internal energy plotted against $\bar{\beta}$ in double-Gaussian approximation (solid line). Kink (dashed line) and nonlinear phonon (dot-dashed line) contributions are shown separately (modulo an irrelevant constant energy shift). Note that kinks dominate over nonlinear phonons in the region where the specific heat has a maximum.

There is a clear indication of an intricate energy sharing mechanism operating between the nonlinear phonons and kinks at intermediate temperatures with kinks dominating the internal energy in the neighborhood of $\bar{\beta} \sim 5.4$. Presumably this is due to the fact that at these temperatures kinks emerge as well defined localized objects and are created with relative ease.

The results from the double-Gaussian approximation as shown in Figs. 7 and 8 are not quantitatively trustworthy for $\bar{\beta} > 5$ as the approximation breaks down at that point. However, we expect them to be correct qualitatively: since this method underestimates the overlap at low temperatures it, in fact, suppresses the kink contribution at lower temperatures. Therefore it is highly unlikely that the peak in the specific heat due to the kink contribution is an artifact of the approximation. A direct comparison of the theoretical results for the specific heat with numerical simulations is possible but requires high statistics. Work in this direction is in progress.

V. DISCUSSION

In summary, we have shown that the dilute-gas or WKB approximation is excellent for $\bar{\beta} > 6$ with no further phonon dressing of the bare kink energy beyond that already included in (11) and (13) at these low temperatures. In particular, we see no evidence of a reduction in the kink mass as suggested in some previous simulations [13–15]. At higher temperatures, the WKB analysis fails, though theoretical progress is possible with the double-Gaussian technique. In this temperature regime, we have shown that the correlation length as measured in the simulations in very good agreement with the theory and that the kink number density, while not being a well-defined quantity, can still be understood at least qualitatively. The double-Gaussian approximation also accurately predicts the onset of short-range order in the system as evidenced by the probability distribution function crossing over from a single- to a double-peaked distribution.

The work reported here contains some of the largest simulations carried out to date on the Φ^4 model. The advantage of size is apparent: we have been able to go to low enough temperatures to unambiguously verify the WKB predictions for this model. Furthermore, the large system size enabled us to check for finite-size effects and to be confident of their absence.

The decomposition of the specific heat into two contributions via the double-Gaussian approximation appears to demonstrate the existence of a nontrivial energy sharing interaction between kinks and nonlinear phonons in the neighborhood of the temperature where the specific heat is a maximum. At this temperature ($\bar{\beta} \sim 5.4$), kinks exist as well-defined objects (Fig. 1) but the dilute-gas or WKB theory is not valid. It would be interesting to see if an analytic study of the thermodynamics of kinks and phonons is possible in a phenomenological theory in this temperature regime.

We expect to apply the double-Gaussian variational method to other problems in the future, e.g., sine-Gordon and Φ^6 field theories in 1+1 dimensions. Work on the Langevin simulation method applied to calculate dynamical correlation functions is already in progress.

[1] See, e.g., A. Seeger and P. Schiller, in *Physical Acoustics*, Vol. III, edited by W. P. Mason (Academic, New York, 1966).

[2] *Solitons and Condensed Matter Physics*, Proceedings of the Symposium on Nonlinear Structure and Dynamics in Condensed Matter, edited by A. R. Bishop and T. Schneider (Springer-Verlag, New York, 1978).

[3] A. R. Bishop, J. A. Krumhansl, and S. E. Trullinger, Physica D **1**, 1 (1980).

[4] V. A. Kuzmin, V. A. Rubakov, and M. E. Shaposhnikov, Phys. Lett. **155B**, 36 (1985).

[5] See, e.g., E. W. Kolb and M. S. Turner, *The Early Universe* (Addison-Wesley, New York, 1990).

[6] A. D. Bruce, in *Solitons and Condensed Matter Physics*,

Ref. [2].

[7] H.-J. Mikeska and M. Steiner, Adv. Phys. **40**, 191 (1991).

[8] J. A. Krumhansl and J. R. Schrieffer, Phys. Rev. B **11**, 3535 (1975).

[9] J. F. Currie, J. A. Krumhansl, A. R. Bishop, and S. E. Trullinger, Phys. Rev. B **22**, 477 (1980).

[10] D. J. Scalapino, M. Sears, and R. A. Ferrell, Phys. Rev. B **6**, 3409 (1972).

[11] T. R. Koehler, A. R. Bishop, J. A. Krumhansl, and J. R. Schrieffer, Solid State Commun. **17**, 1515 (1975).

[12] D. Yu Grigoriev and V. A. Rubakov, Nucl. Phys. B **299**, 67 (1988).

[13] A. I. Bochkarev and Ph. de Forcrand, Phys. Rev. Lett. **63**, 2337 (1989).

[14] M. Alford, H. Feldman, and M. Gleiser, Phys. Rev. Lett. **68**, 1645 (1992).

[15] A. Krasnitz and R. Potting (unpublished).

[16] F. Marchesoni, Phys. Rev. Lett. **64**, 2212 (1990).

[17] A. I. Bochkarev and Ph. de Forcrand, Phys. Rev. Lett. **64**, 2213 (1990).

[18] E. Stoll, T. Schneider, and A. R. Bishop, Phys. Rev. Lett. **42**, 937 (1979).

[19] F. J. Alexander and S. Habib, Phys. Rev. Lett. **71**, 955 (1993).

[20] T. Schneider and E. Stoll, Phys. Rev. B **22**, 5317 (1980).

[21] A. R. Bishop and J. A. Krumhansl, Phys. Rev. B **12**, 2824 (1975).

[22] See, e.g., P. M. Stevenson, Phys. Rev. D **30**, 1712 (1984).

[23] A. D. Bruce, Adv. Phys. **29**, 111 (1980).

[24] A. R. Bishop, in *Lattice Dynamics,* Proceedings of the International Conference on Lattice Dynamics, Paris, 1977, edited by M. Balkanski (Flammarion Sciences, Paris, 1978).